



**HAL**  
open science

# Nylon/Ag fiber sensor for real-time damage monitoring of composites subjected to dynamic loading

Yumna Qureshi, Mostapha Tarfaoui, Hamza Benyahia, K. K. Lafdi

## ► To cite this version:

Yumna Qureshi, Mostapha Tarfaoui, Hamza Benyahia, K. K. Lafdi. Nylon/Ag fiber sensor for real-time damage monitoring of composites subjected to dynamic loading. *Smart Materials and Structures*, 2020, 29 (11), pp.115045. 10.1088/1361-665X/abb646 . hal-02995617

**HAL Id: hal-02995617**

**<https://ensta-bretagne.hal.science/hal-02995617>**

Submitted on 25 Jun 2021

**HAL** is a multi-disciplinary open access archive for the deposit and dissemination of scientific research documents, whether they are published or not. The documents may come from teaching and research institutions in France or abroad, or from public or private research centers.

L'archive ouverte pluridisciplinaire **HAL**, est destinée au dépôt et à la diffusion de documents scientifiques de niveau recherche, publiés ou non, émanant des établissements d'enseignement et de recherche français ou étrangers, des laboratoires publics ou privés.



Distributed under a Creative Commons Attribution 4.0 International License

# Nylon/Ag fiber sensor for real-time damage monitoring of composites subjected to dynamic loading

Y Qureshi<sup>1</sup> , M Tarfaoui<sup>1,2</sup> , H Benyahia<sup>1</sup>, K K Lafdi<sup>2</sup> and K Lafdi<sup>2,3</sup>

<sup>1</sup> ENSTA Bretagne, IRDL - UMR CNRS 6027, F-29200, Brest, France

<sup>2</sup> University of Dayton, Nanomaterials Laboratory, Dayton, OH 45469-0168, United States of America

<sup>3</sup> Department of Mechanical and Construction Engineering, Northumbria University, Newcastle upon Tyne, United Kingdom

E-mail: yumna.qureshi@ensta-bretagne.org and mostapha.tarfaoui@ensta-bretagne.fr

In this article, the goal is to monitor the deformation and damage behavior of composites in real-time using a Nylon/Ag fiber sensor when subjected to dynamic loading. Composite samples are integrated with Nylon/Ag fiber sensors at distinct locations and directions between the plies. Then, these samples are experimentally impacted with low-velocity impact using the Taylor Cannon Gun apparatus at three different velocities i.e.  $2.5 \text{ ms}^{-1}$ ,  $3 \text{ ms}^{-1}$ , and  $6.5 \text{ ms}^{-1}$ , respectively. These three sets of tests are conducted to determine the detection performance of the Nylon/Ag fiber sensor when the composite sample experiences no damage, some microdamage, and overall breakage. Besides, the fiber sensor placed in each position showed distinct electrical behavior in all three tests and detected the deformation, damage initiation, quantification, identification, and damage propagation. The results confirmed the ability of the fiber sensor to monitor and identify the mechanical deformation during dynamic loading and showed that the sensor can be used as a flexible sensor reinforcement in composites for *in-situ* monitoring as well.

Keywords: composites, dynamic loading, damage behavior, real-time monitoring, fiber sensor

## 1. Introduction

Even though vast research has been going to monitor deformation and damage in real-time during quasi-static loading but monitoring systems for dynamic failure are still underdeveloped. The impact such as hailstone, bird strike, and other mechanical collisions were some of the frequent dynamic loadings for structures such as wind turbines, aircraft and bridges which could affect the integrity of the structure and induce fiber breakage, delamination, matrix cracking or interfacial failure [1–3]. Moreover, impact loading was one of the most common causes of the failure of structure and it was often very difficult to detect failure because damage occurs very fast and generally not visually visible [4–7].

Structural health monitoring (SHM) is a widely known phenomenon to monitor the health of the structure in real-time so, the failure can be sensed before the final failure of the structure [8]. Detection of impact damage was usually conducted after the impact with non-destructive testing techniques such as ultrasonic [9], acoustic emission [10–13], fiber Bragg grating (FBG) [14, 15], optical fiber [16]. However, these techniques were expensive, difficult to install, prone to external noise, and required complex installation procedure [17, 18]. The studies conducted to detect the damage during impact dynamic loading were mostly focused on the damage detection and did not include the study of detection signal to elaborate the monitoring of deformation, damage initiation, damage propagation, damage quantification, and identification of

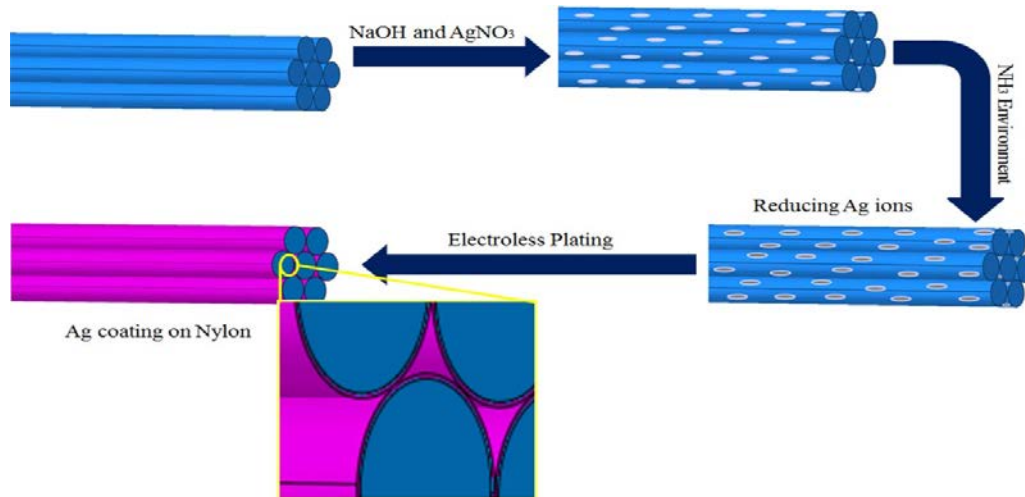


**Figure 1.** Manufacturing process of Nylon/Ag fiber sensor.

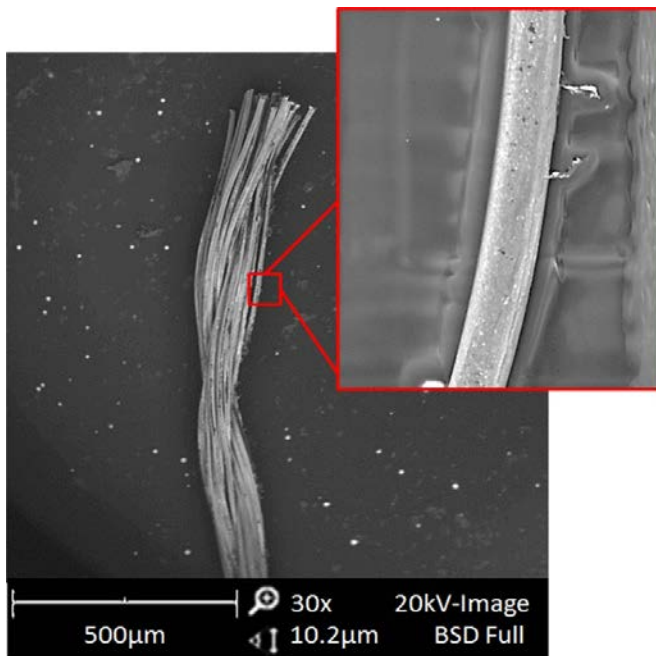


**Figure 2.** SEM characterization of Nylon/Ag fiber sensor after manufacturing.

the type of damage. This limitation was the main motivation behind this research.

The change in measurement of the electrical resistance (ER) was one of the real-time SHM methods that were used to monitor the behavior of composite samples during working conditions, specifically for carbon fibers composites for their good electrical and thermal conductivity [19–22]. It worked based on the rearrangement of carbon fibers and contact point change within composites during failure [23–31]. However, this method was unfavorable for low conductive composites such as glass fiber or cementitious composites which required

the addition of nanofillers [32–37] for their self-sensing behavior by enhancing their electrical behavior during operation [38–43]. However, the addition of nanofillers could not be applied on large scale structures because high mass fractions of the nanofillers will be needed to ensure good conductance that could cause an increase in cost and difficulty in uniform dispersion [44, 45].

Smart textiles were then considered as a promising alternative for the SHM application because they can behave as reinforcement and monitor the mechanical behavior of the structural component simultaneously [46–48]. Fabrics, yarns, and other textiles are some of the examples of these conductive fiber sensors which work on the basic principle of traditional strain gauges [49]. Initially, conductive polymers were considered for real-time damage monitoring however, they were affected by the environmental factor and their conductance was less in comparison with the nanoparticles [50, 51]. Therefore, integrating the polymer textiles or coating them with conductive nanoparticles such as graphene nanoplatelets (GNP) and carbon nanotubes (CNTs) were considered for real-time SHM of structural components [52–56]. However, the porous network of CNTs and their tunneling effect resulted in affecting the sensitivity of CNT based sensors [57–60] while GNP had stability issues in exposed air and it is also toxic [61, 62].

Furthermore, metal nanoparticles were also considered for real-time damage monitoring applications. Amongst all metal nanoparticles, silver (Ag) showed promising results when used as a coating for flexible substrates like yarns and other polymer textiles because of its good mechanical performance, thermal behavior, electrical properties, competitive price, and stability in air [62–69]. However, the use of these Ag coated smart textiles in SHM of composites under dynamic loading is still limited. Recently, Y Qureshi *et al* [69, 70] studied Nylon/Ag fiber sensor as a strain sensor for real-time SHM of composites under quasi-static elongation and displayed that the location of sensor plays a significant part in identifying the type of damage [71]. Moreover, they also studied that the position of

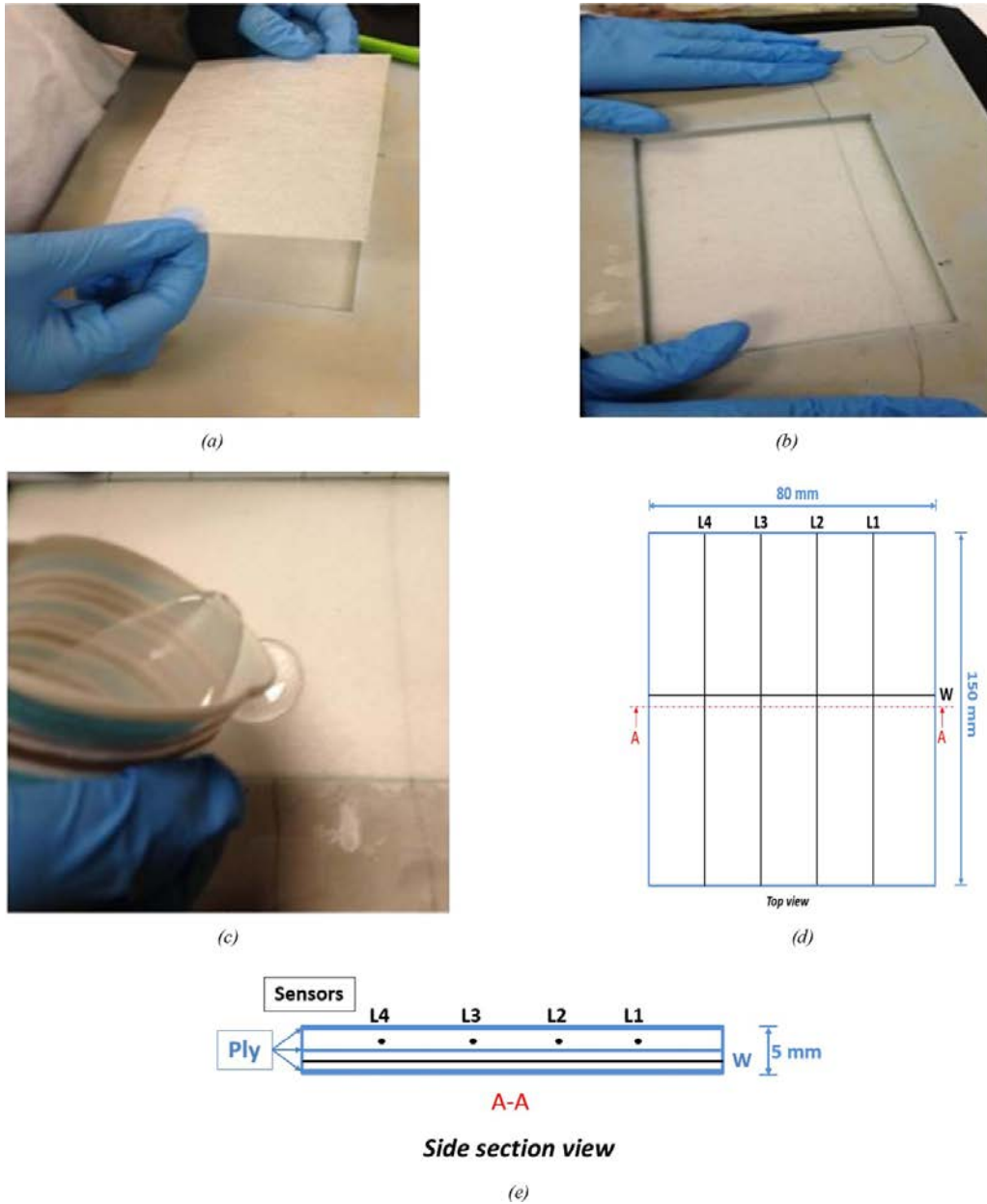


**Figure 3.** (a)–(c) Composite sample preparation process with integration of Nylon/Ag fiber sensors (d)–(e) Geometric parameters of the samples and placement of Nylon/Ag fiber sensor in each position correspondingly.

the sensor played a vital role in detecting the type and amount of damage in composites during flexural loading [72, 73]. However, up to the best knowledge of the author, there is no or limited information available regarding the use of smart textiles for dynamic damage monitoring in real-time. Moreover, the studies conducted to detect the damage during impact dynamic loading were mostly focused on the damage detection and did not include the study of detection signal to elaborate the monitoring of deformation, damage initiation, damage propagation, damage quantification and identification of the type of damage. This limitation was the main motivation behind this research.

Hence, in this study, an investigation was carried out to observe the ability of the Nylon/Ag fiber sensor to monitor the mechanical behavior of composite material in real-time under dynamic impact. Besides, the ability of the fiber sensor to distinguish between different types of failures and quantification of induced damage was also studied by placing the fiber sensor in different positions. The fiber sensor was inserted in the composite plate sample in their particular direction and position during the manufacturing process. Then each composite plate sample was tested experimentally on TAYLOR GUN under low-velocity impact and its deformation was monitored by correlating its mechanical behavior

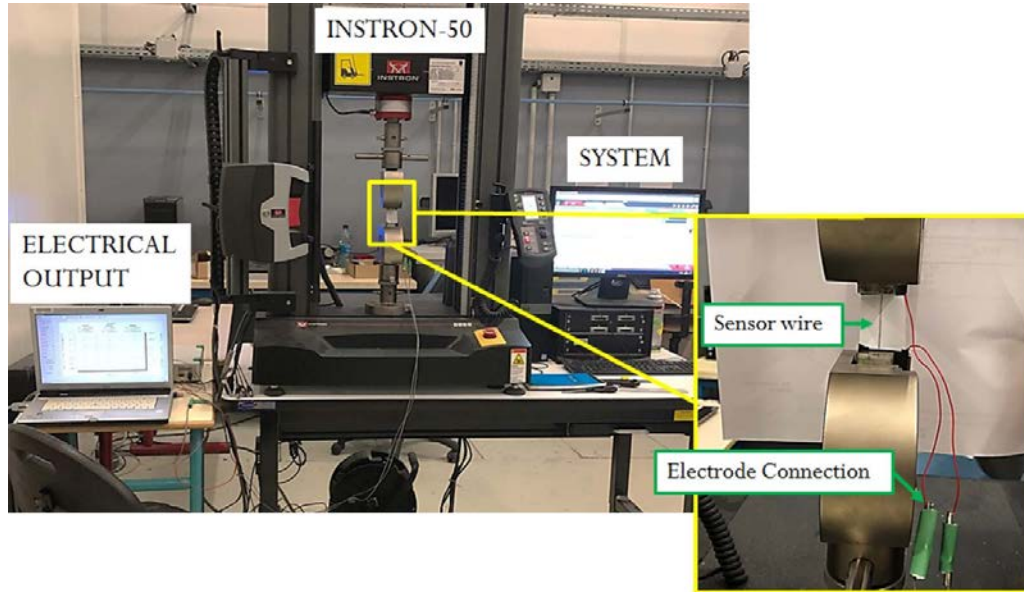


**Figure 4.** Experimental setup to calculate the Gauge Factor of the fiber sensor.

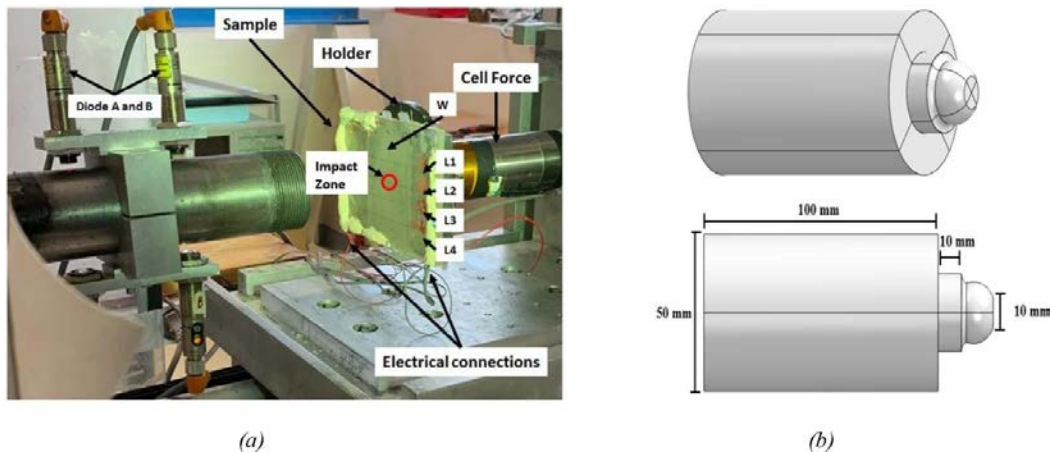


**Figure 5.** Experimental setup to inspect the real-time monitoring behavior of the Nylon/Ag fiber sensor within the composite under dynamic impact.

with the electrical behavior of fiber sensor in each position. The results presented exciting performance and showed that the fiber sensor monitored the deformation and established that the position of the fiber sensor played a vital role in differentiating between different types of damage and in quantifying them. Moreover, the sensor showed good potential to monitor damage in dynamic failure and to detect damage propagation phenomenon throughout the sample.

## 2. Sample preparation

Nylon/Ag fiber sensor was fabricated using an electroless plating process to deposit a continuous coating of Ag nanoparticles on the surface of filaments of nylon yarn. The electroless plating process was utilized because of its simplicity and effectiveness for complex geometries [69, 70],

figure 1. Scanning electron microscopy (SEM) image showed uniform and continuous coating of nylon yarn with Ag nanoparticles [69, 70], figure 2. Afterward, Nylon/Ag fiber sensor was embedded within the three plies of chopped glass fiber mat in their particular location and direction during the manufacturing of the plate sample and these plies separated the fiber sensor from each other, figure 3(a). Also, the poor conductivity of the glass fiber mat ensured electrical isolation of the sensor in each position, and randomly oriented chopped fibers confirmed the isotropic behavior of the sample. Four sensors were placed along the length of the composite sample between ply 2 and 3 at position  $L_1$ ,  $L_2$ ,  $L_3$ , and  $L_4$  while one Nylon/Ag fiber sensor was integrated between the ply 1 and ply 2 in the position along the width of the sample and the center i.e.  $W$ , figure 3(b). After the addition of 1:4 ratio of resin and hardener blend into the mold, composite samples were cured for 48 h at room temperature and full integration of the sensors

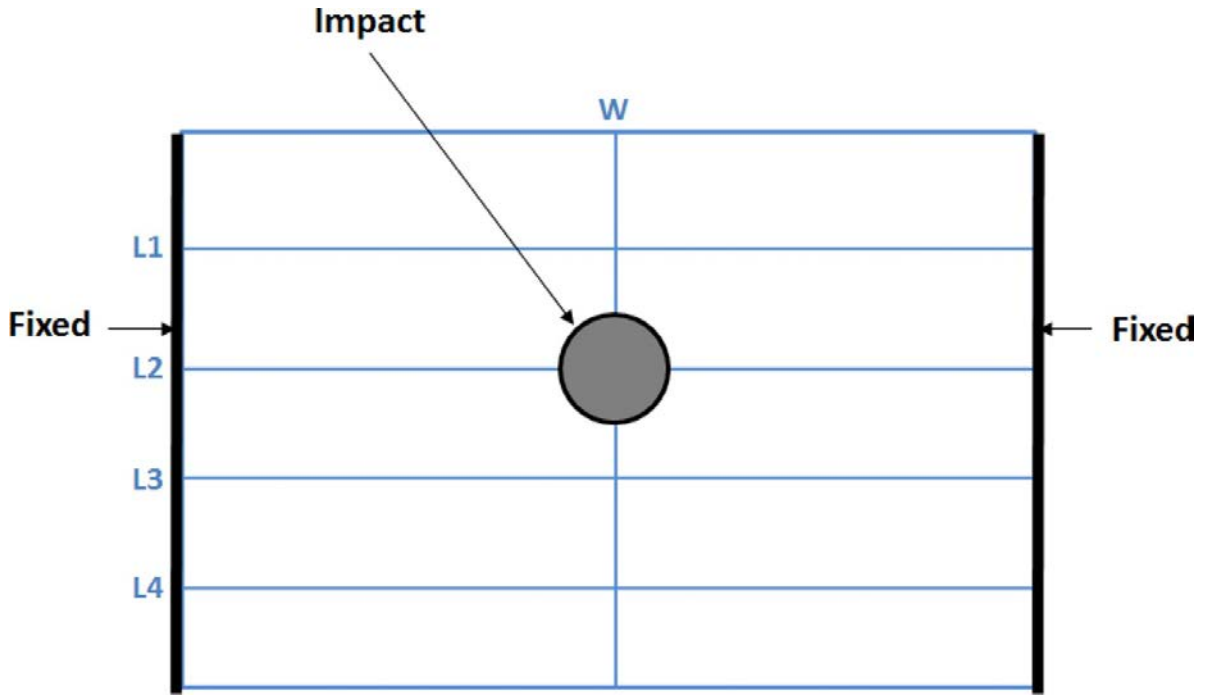


Figure 6. Experimental boundary conditions and position of impact.

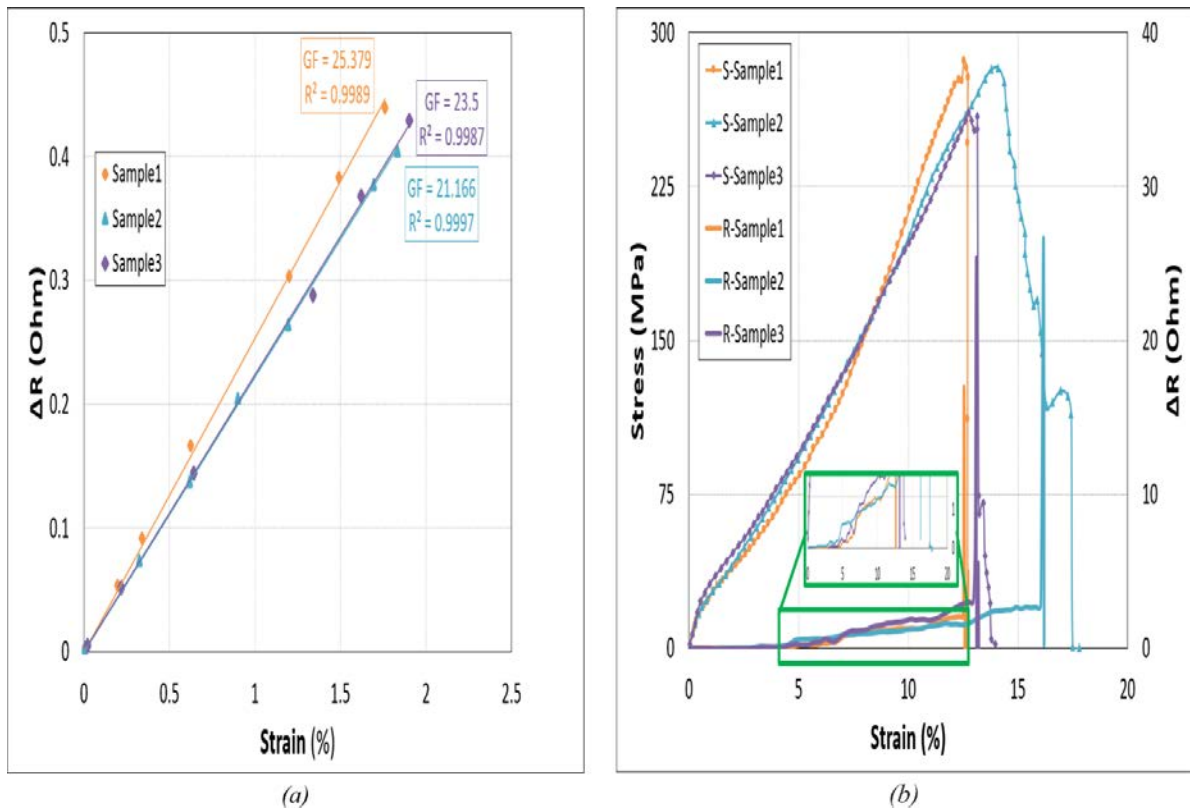


Figure 7. Experimental calculation of the sensitivity of the Nylon/Ag Fiber sensor.

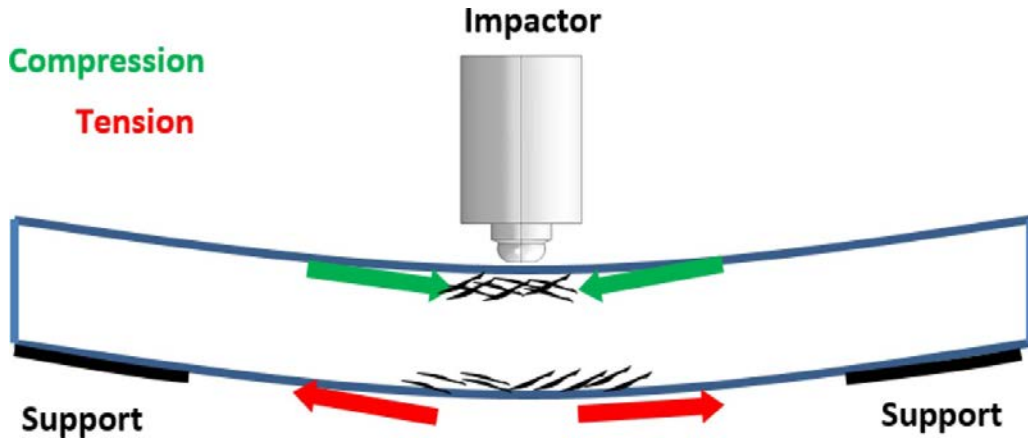


Figure 8. Deformation mechanism of the composite sample during the impact.

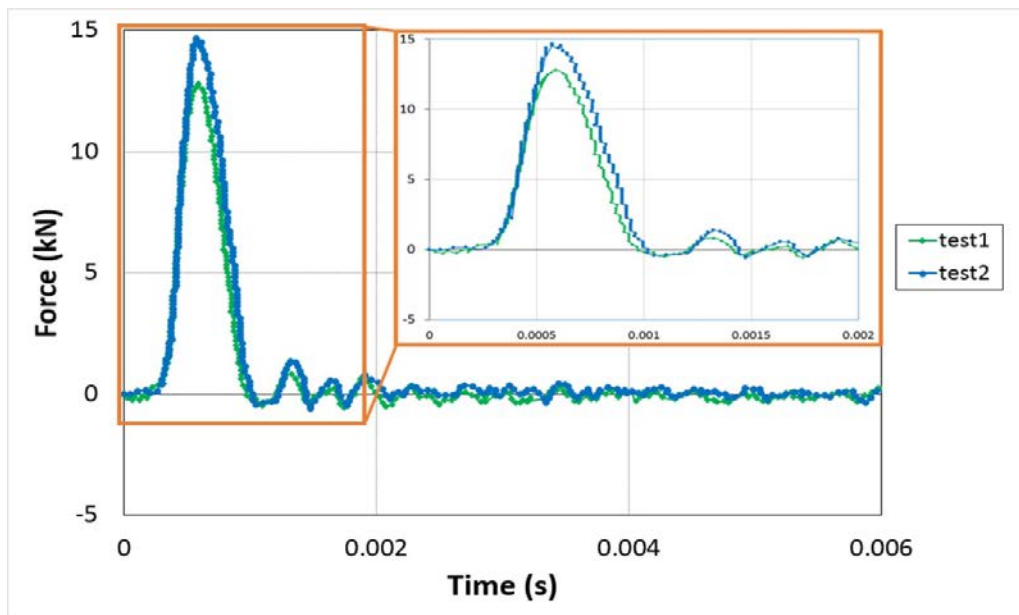


Figure 9. Comparison of experimental behavior of the first two tests which were without any visible macro damage.

was attained in each sample, figure 3(c). Each sample was of 5 mm in thickness, 80 mm in width and 150 mm in length and geometric demonstration of the sample clarified the direction and location of the Nylon/Ag fiber sensor within the sample, figures 3(d)–(e).

### 3. Experimental procedure

Nylon/Ag fiber sensor was tested as a standalone sensor to demonstrate its strain sensitivity by calculating its gauge factor and this procedure is discussed in detail in [70], figure 4. Composite plate embedded with the Nylon/Ag fiber sensors was experimentally tested under low-velocity impact using the Taylor Cannon Gun. Electrical signals of the Nylon/Ag fiber sensors, placed at different positions within the sample, were recorded using the data acquisition system (manufactured by HBM) for monitoring the mechanical behavior of the

sample in real-time, figure 5(a). The sample was placed on the holder with precaution to ensure electrical isolation of all electrical connections from any metallic part of the machine to avoid any perturbation in the signal of the sensors. Afterward, the specimens were tested at a low-velocity impact range with an impactor of 1.6 kg, and diodes were used to record the velocity of the impactor, figure 5(b). Three sets of tests were performed to examine the detection behavior of the fiber sensors. The first test was performed at  $2.5 \text{ m s}^{-1}$  and while the second test was performed at  $3 \text{ m s}^{-1}$  and in each set of tests sample was impacted at the position shown in figure 6. This position was selected to ensure the maximum possibility of distinct behavior of the sensor in each position to demonstrate the complex failure mechanism of the composite sample under dynamic loading. The first two tests were performed to observe the real-time detection response and sensitivity of the designed Nylon/Ag fiber sensor where there is elastic deformation or some localized permanent deformation at the

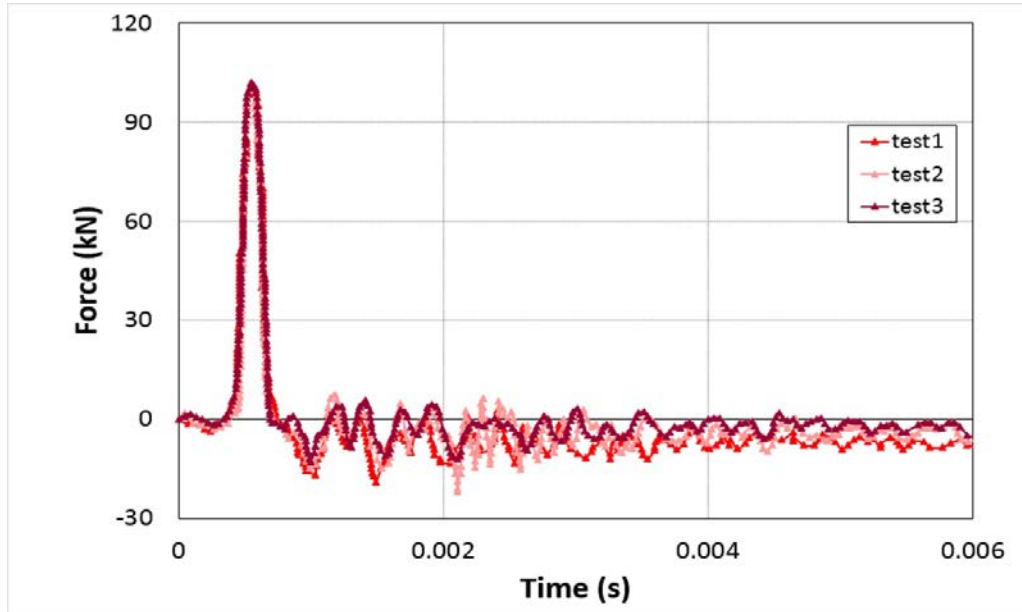


**Figure 10.** Mechanical behavior of fractured composite sample and repeatability of mechanical results. Test 1 was performed on the sample integrated with fiber sensors and test 2 and test 3 were performed on sample without fiber sensors.

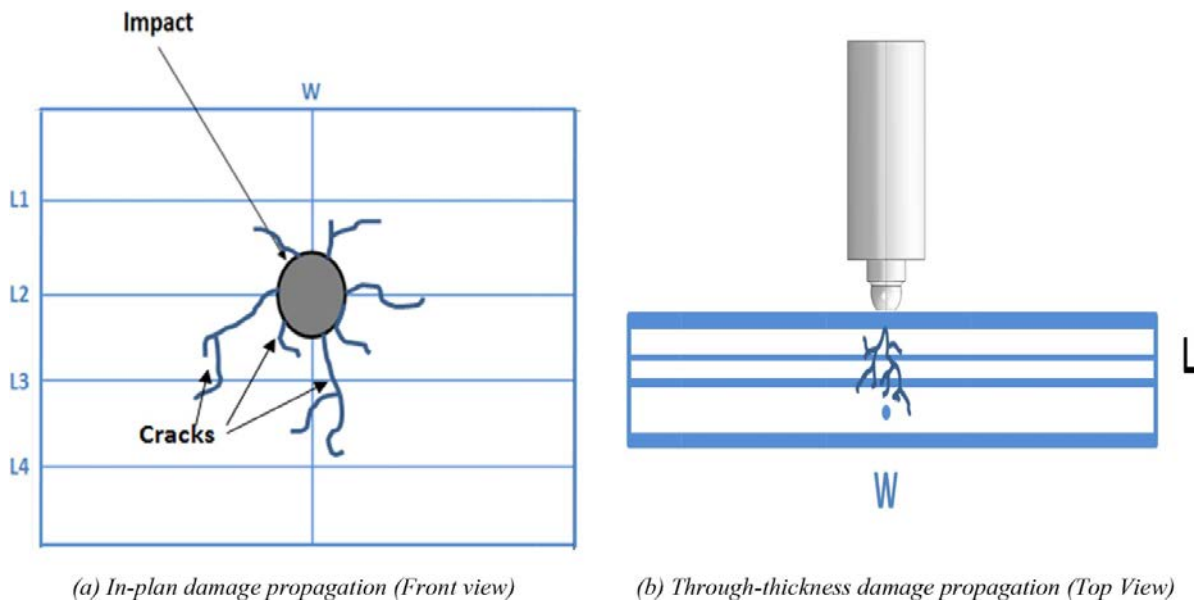


**Figure 11.** Overall fracture and damage propagation during the impact of composite plate. (a) In-plan damage propagation (Front view). (b) Through-thickness damage propagation (Top View).

microscale and the position of impact was selected to demonstrate the detection of damage propagation. The third set of tests was performed at  $6.5 \text{ m s}^{-1}$  to ensure overall damage and final fracture of the samples and samples were impacted in the same position as the first two tests. It must be kept in mind that this investigation was conducted to understand the real-time damage detection behavior of sensors during dynamic loading when inserted into the composite which could be subjected to variable damage behavior. However, three tests were conducted for overall damage and fracture of the specimen to show the repeatability of the mechanical response of the composite specimen. Two specimens were tested without fiber

sensors and one was tested with the integrated fiber sensors at different locations.

## 4. Results and discussions

### 4.1. Strain sensitivity of the Nylon/Ag fiber sensor

The gauge factor (G.F) was calculated to demonstrate the strain sensitivity of the fiber sensor by comparing the change in resistance  $\Delta R/R_o$  of the sensor against the applied strain  $\epsilon$

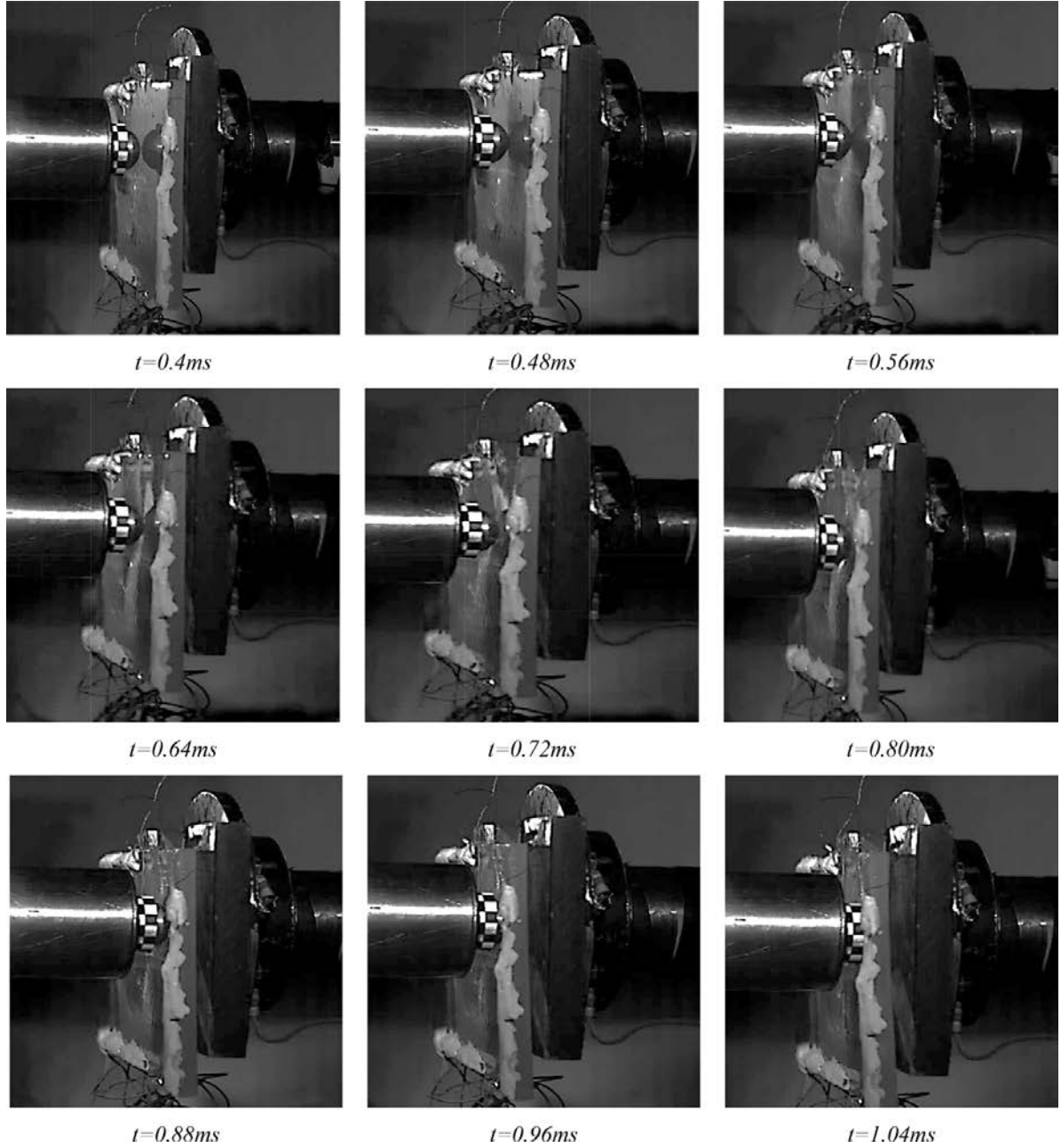


**Figure 12.** Real-time high-speed photographs of dynamic impact test performed at  $v = 6.5 \text{ m s}^{-1}$  on the composite sample.

as shown in equation (1).

$$G.F = \frac{\left(\frac{\Delta R}{R_0}\right)}{\varepsilon} \quad (1)$$

The G.F was found to be in the range of 21–25 within the elastic limit, figure 7(a). Moreover, overall electromechanical behavior of each specimen also showed good correlation by demonstrating linear gradual increase in the resistance with the applied strain. The resistance achieved its maximum value upon the damage, figure 7(b).

#### 4.2. Mechanical behavior of composite sample

It was necessary to understand the mechanical behavior of the composite under dynamic impact to apprehend the detection behavior of the Nylon/Ag fiber sensor. The sample was fixed on the two opposite sides and was impacted in the center. During the impact, the sample experienced compression deformation at the upper surface which was in direct contact with the impactor while lower surface experienced tensile stress in response to the compression strain similar to the failure mechanism of the sample subjected to flexural bending [72], figure 8. The first two tests performed at  $2.5 \text{ m s}^{-1}$  and  $3 \text{ m s}^{-1}$  respectively showed similar overall mechanical response with a slight increase in the overall force because of

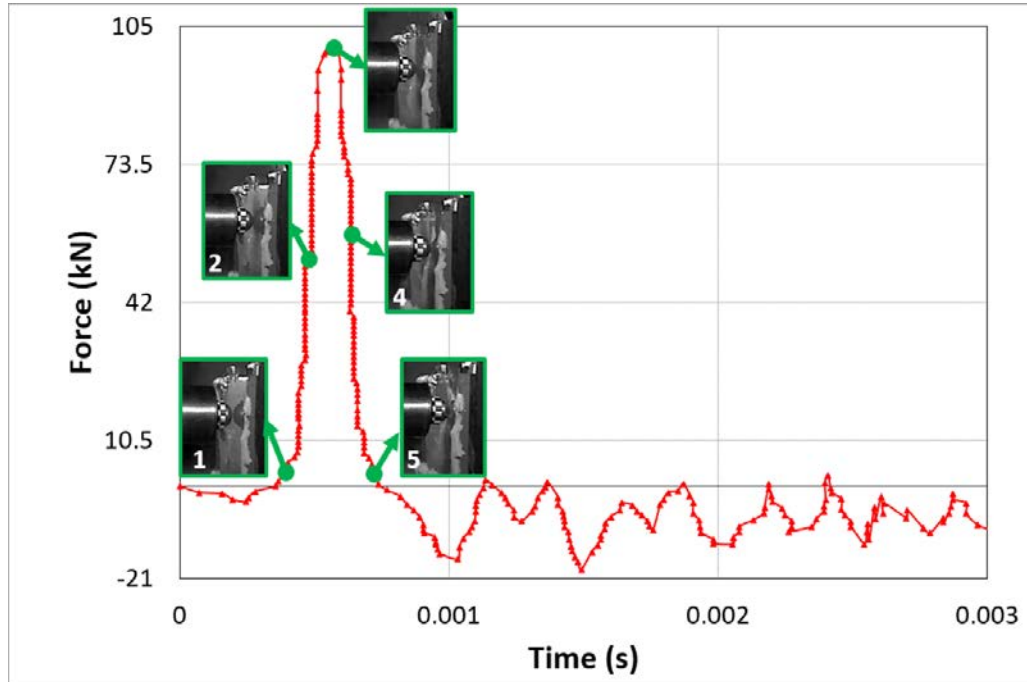


**Figure 13.** Mechanical behavior and high-speed camera images of a test performed at an impact velocity of 6.5 m/s.

the increase in the impact velocity, figure 9. The maximum force at 2.5 m s<sup>-1</sup> and 3 m s<sup>-1</sup> are respectively 12.089 kN and 14.678 kN respectively. Then, three tests were performed at 6.5 m s<sup>-1</sup> and they displayed good repeatability in the mechanical behavior of the composite samples, figure 10. During the test at 6.5 m s<sup>-1</sup>, the damage propagation occurred within the plies and through thickness which led to the overall fracture of the composite plate, figure 11. High speed camera was also used to monitor the behavior of the plate during the impact and verify the damage mechanism, figure 12. Comparison of the high-speed camera images with the mechanical behavior of the composite plate showed that the samples were completely fractured at this impact velocity frame by frame, figure 13.

#### 4.3. SEM characterization of fractured sample

SEM was also carried out of the fractured sample to understand the damage and fracture behavior of the sample and to identify the position of the respective fiber sensors. It was visible in the SEM image that the sample consisted of three plies, figures 14(a) and (b). It also identified the randomly oriented chopped fibers and epoxy in each ply. Moreover, cracks and damage propagation were also visible in the SEM images and one of the interesting things observed was that none of the crack initiation and damage propagation was found near the region of integration of the Nylon/Ag fiber sensor, figures 14(c) and (d). This concluded that this fiber sensor monitored the sample in real-time and did not act as a defect [72]. In addition, SEM images also showed the placement of fiber sensors in different positions, for example, two fiber sensors are perpendicular to

each other and in different plies were seen in this respective image, figure 14(e). One of the fiber sensors was in position W and the other one could be anyone from the fiber sensors placed in  $L_1$ ,  $L_2$ ,  $L_3$ , and  $L_4$ . Coated filaments of Nylon/Ag fiber sensors were visible when SEM characterization was carried out at higher magnification, figure 14(f). Some of the filaments of the broken fiber sensor (during the fracture) also showed removal of coating in some regions and one can distinguish the nylon core from the Ag coating, figure 14(f).

#### 4.4. Real-time damage monitoring by Nylon/Ag fiber sensor

The first sample tested at an impact velocity of 2.5 m s<sup>-1</sup>, was to determine the deformation detection by the Nylon/Ag fiber sensor. The electrical response of the sensor correlated perfectly with the mechanical behavior of the composite. Sample was impacted at the position described in section 3 and three very interesting phenomena were observed during the dynamic deformation. The result showed that when the sample was impacted with the impactor there was sudden and quick decrease in the resistance of the sensor placed in  $L_2$  and then it returned to the original behavior, figure 15. The first phenomenon showed that the damage was local and was only detected by the sensor beneath or closer to the impacted region i.e.  $L_2$  and fiber sensor placed in all the other positions did not show any change of behavior. The second phenomenon was that the fiber sensor showed a decrease in resistance which confirmed the presence of compressive strain during the impact which was logical because the surface of the material in direct contact of the impactor experienced compression deformation. The third phenomenon was the return of the ER

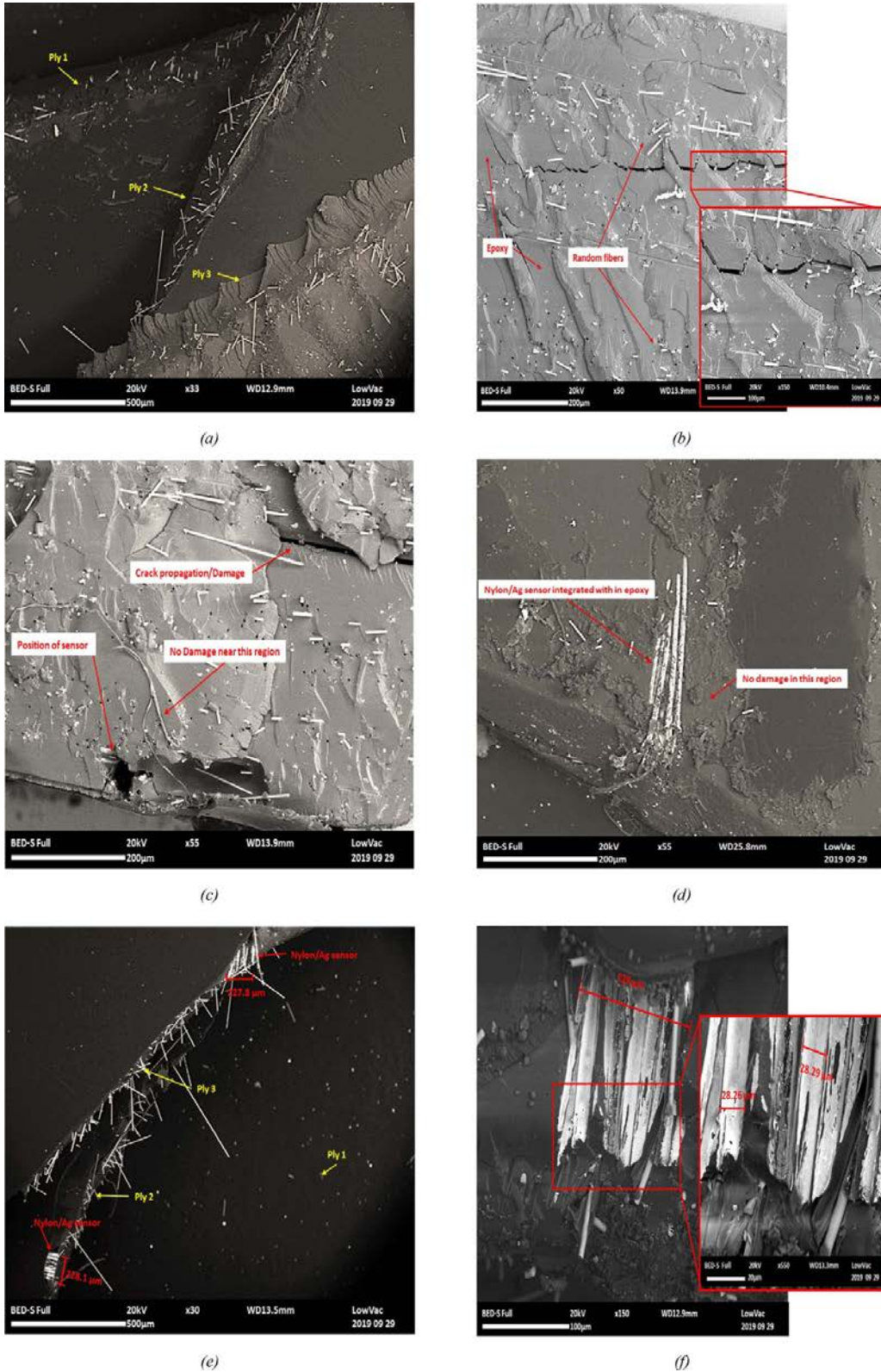


**Figure 14.** SEM characterization of fractured sample. (a) shows the distinct three plies of the composite specimen with randomly oriented chopped fibers (b) shows epoxy and fibers at higher magnification with the presence of a crack (c)-(d) show the positions where Nylon/Ag fibers were placed during the fabrication and no damage was found near these regions. These two images were taken at two different coordinates (e) demonstrate two Nylon/Ag fiber sensors placed perpendicular to each other and within different plies (f) shows Nylon/Ag fiber sensor at higher magnification.

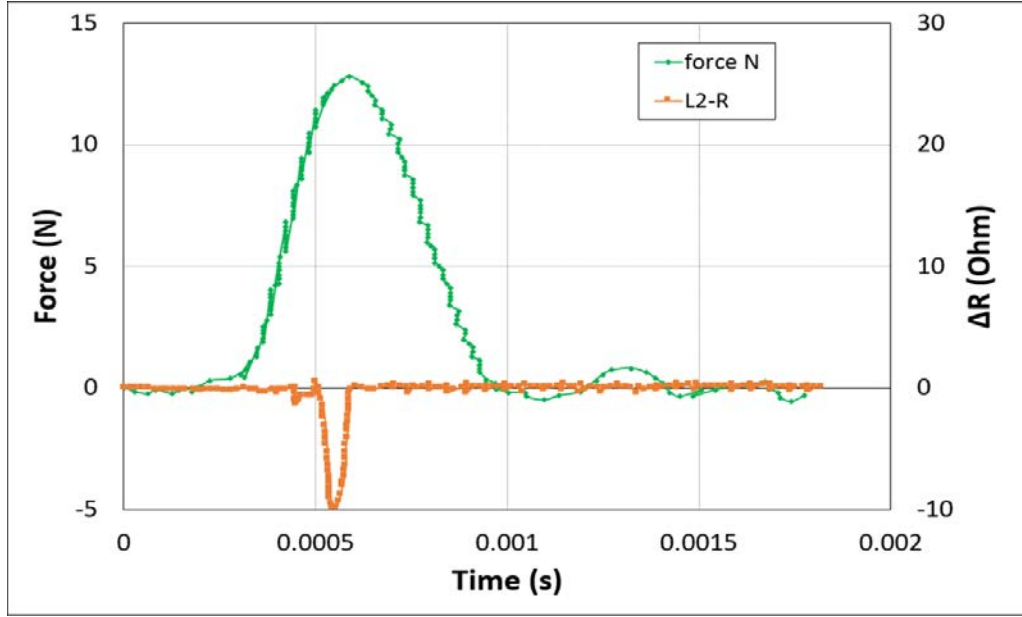


**Figure 15.** *In-situ* detection of deformation in the composite sample under dynamic impact at  $v = 2.5 \text{ m s}^{-1}$  by Nylon/Ag fiber sensor.

to the original signal which showed that there was no permanent damage or damage propagation and the material recovered all the compressive strain induced by the impactor. Furthermore, this test confirmed the ability of the Nylon/Ag fiber sensor to detect the deformation of the sample or its damage behavior in real-time with good accuracy during dynamic impact.

The second sample was tested at the same position but with slightly higher velocity to induce certain permanent damage in the sample without breakage to recognize the behavior of the Nylon/Ag fiber sensor when there is permanent damage and damage propagation. The results showed that sensors in positions  $L_2$ ,  $L_3$ , and  $W$  showed a change in resistance while fiber sensors in  $L_1$  and  $L_4$  positions did not show any change in the signal, figure 16. This confirmed that the damage was local and did not propagate on a larger scale. The signal of fiber sensor in positions of  $L_2$ ,  $L_3$ , and  $W$  confirmed that the damage propagation was not only in-plane but also through the thickness which confirmed the presence of internal permanent damage whether it was micro or macro in scale. The results of this test showed another important phenomenon, the delay in the change of resistance of each sensor which demonstrated the time taken by the damage to propagate and reach to the region where there was another fiber sensor and this delay was recorded in milliseconds. Furthermore, the unique behavior of fiber sensor in each position displayed the detection of different type of damage, for example, decrease in the resistance of fiber sensor in  $L_2$  and  $L_3$  positions showed the presence of compressive damage in the area which was in direct contact or closer to the impact, however, increase in the resistance of the fiber sensor in  $W$  position showed the presence of tensile damage in the lower surface of the specimen.

Another interesting behavior observed in the signal of these fiber sensors during the deformation was that the fiber sensors in all three positions showed the different intensity of signal

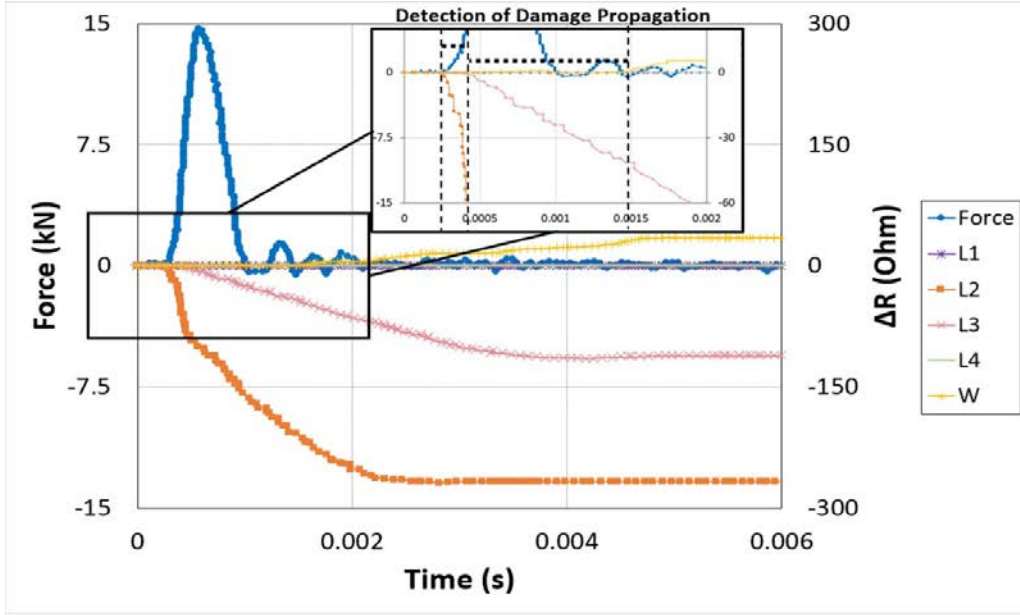
change and all of them did not return to the original signal. The permanent change in the signal of the sensor confirmed the presence of permanent damage or deformation which the difference in the intensity of the signal quantified the amount of damage in the respective regions. For example, fiber sensor in  $L_2$  position showed more increase in resistance than in  $L_3$  position because the  $L_2$  position was closer to the impacted region and experienced maximum effect of the damage while the fiber sensor in  $W$  position experienced the minimum effect because damage propagation was more favorable within the ply and traveled faster in comparison to propagating through-thickness.

This test confirmed the ability of the said monitoring system to not only detect the damage propagation but also to quantify different types of damage. To further explain the quantification of damage, linear empirical equations accurately describe the relation of the change in resistance with the damage rate within the composite sample. These empirical relations were derived from the curves in figure 16(b) and showed a linear change in the resistance (Ohm) with respect to the time (s). Two equations were derived, one for the positive change in resistance ( $R_P$ ) and one for the negative change in resistance ( $R_N$ ) of the sensor with respect to the time. These equations are presented as follow:

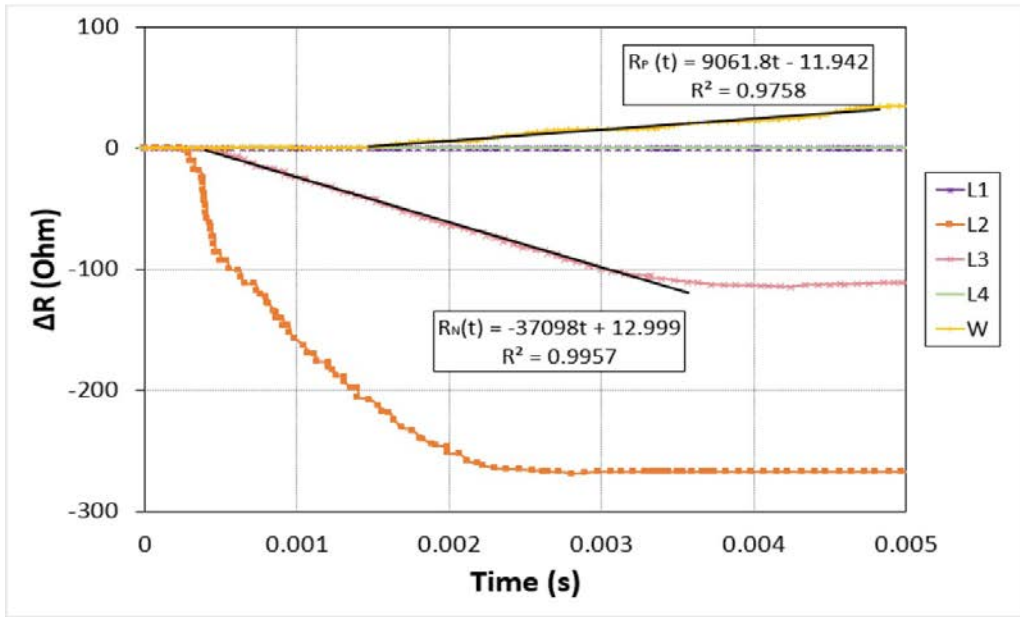
$$\begin{aligned} R_P(t) &= 9061.8t - 11.942 \\ R^2 &= 0.9758 \end{aligned} \quad (2)$$

$$\begin{aligned} R_N(t) &= 37098t + 12.999 \\ R^2 &= 0.9957 \end{aligned} \quad (3)$$

Both equations represented similar empirical relations with an accuracy of 98% which further verified the behavior of



(a)



(b)

**Figure 16.** (a) *In-situ* monitoring in the composite sample by Nylon/Ag fiber sensor subjected to dynamic impact at velocity  $3 \text{ m s}^{-1}$ . (b) Calculation of empirical relations to describe the nonlinear change in resistance with respect to time.

sensors for the quantification of damage. The relation of With resistance with time could be generalized as follow:

$$R(t) = at + b \quad (4)$$

where  $a$ ,  $b$ ,  $c$ ,  $d$ ,  $e$ , and  $f$  are empirical constants.

Now, to quantify the damage rate within the composite sample, we will use the following relation:

$$GF = \frac{\Delta R/R}{\varepsilon} \quad (5)$$

$$R' = \frac{\Delta R}{R} \quad (6)$$

$$\varepsilon = R' * \left( \frac{1}{GF} \right)$$

where GF is the gauge factor constant of the sensor,  $R$  is the original resistance of the sensor, and  $\Delta R$  is the change in the resistance of the sensor with the applied strain  $\varepsilon$ .

By substituting equations (3) in (5), the change of resistance with respect to time can give us change in strain with respect

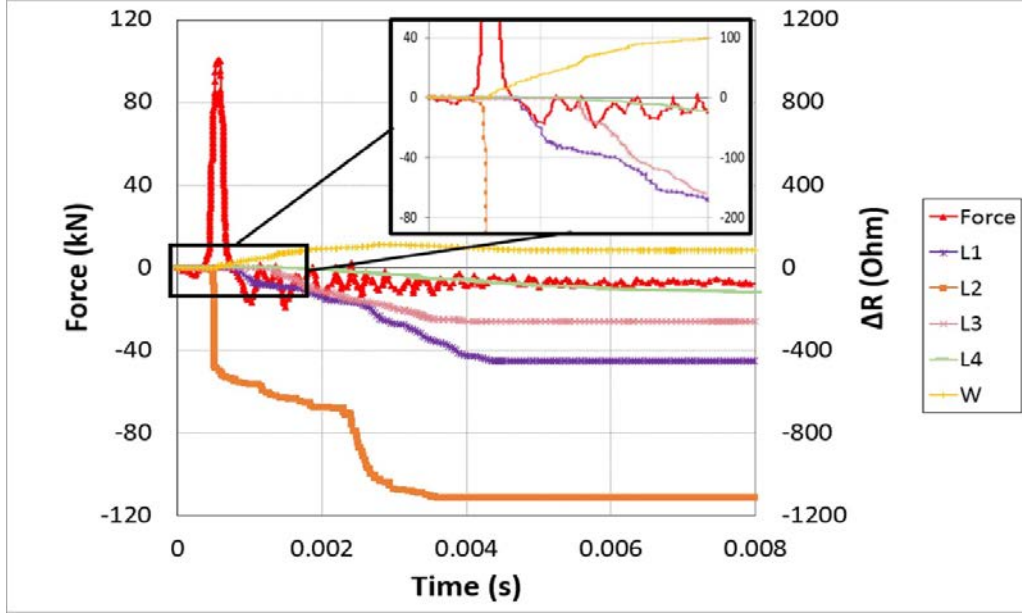


**Figure 17.** *In-situ* monitoring in the composite sample by Nylon/Ag fiber sensor subjected to dynamic impact at velocity  $6.5 \text{ m s}^{-1}$ .

to time i.e. damage rate during dynamic deformation of the composite specimen.

$$\varepsilon(t) = R'(t) * \left( \frac{1}{GF} \right) \quad (7)$$

This equation quantifies the strain rate or damage rate in the composite specimen under dynamic loading using the change in resistance of the signal of the Nylon/Ag fiber sensor in real-time.

Furthermore, the Nylon/Ag fiber sensors inserted in the specimens tested at a velocity of  $6.5 \text{ m s}^{-1}$  for the overall fracture and breakage showed a change in resistance in all positions. They further confirmed the phenomena discussed in the previous two sets of tests in addition, the fiber sensor in all the positions reached their maximum resistance to show the final damage depending upon the amount of damage detected. As usual, the fiber sensor in the  $L_2$  position showed a change in resistance before all the other positions and showed a maximum decrease in resistance during fracture of the specimen which confirmed the presence of maximum cracks and damage near and in the impact zone, figure 17. Fiber sensor in position  $L_1$  also showed a decrease in resistance with less intensity than the fiber sensor in position  $L_2$  and with a slight delay in the signal which was less than 1 ms. This confirmed the damage propagation from position  $L_2$  to  $L_1$  however, the amount of damage in position  $L_1$  was less than  $L_2$  before final failure. The Nylon/Ag fiber sensors placed in the position  $L_3$  and  $L_4$  showed similar response like position  $L_1$  but their intensity of the signal of lower depending upon their distance from the impact zone. The fiber sensor in position  $W$  showed the maximum increase in the resistance before the final fracture indicating the tensile damage but the intensity of the signal confirmed the presence of localized damage. Moreover, it was seen in the results that the delay in the change of signal was

maximum for fiber sensor in position  $L_4$  because of the extended distance and it would have taken more time for the damage to propagate there. In fact, damage propagated first to  $L_1$ , then to  $W$ , then to  $L_3$ , and  $L_4$  position because the distance through-thickness was less than the position  $L_3$  and  $L_4$ . Furthermore, this test helped in understanding the complex damage initiation and propagation behavior in the isotropic composite plate before the final overall fracture.

## 5. Conclusion

In this article, experimentation was carried out to comprehend and examine the detection performance of the Nylon/Ag fiber sensor for monitoring the behavior of the composite plate and its damage evolution under dynamic loading. The fiber sensor was inserted at distinct positions and directions in the composite sample to study its detection behavior and to understand the damage mechanism of the composite sample. The results showed good repeatability in the mechanical performance of the sample and change in electrical behavior of the fiber sensor correlated perfectly with the deformation of the composite plate under low-velocity dynamic impact. Moreover, the fiber sensor placed in each position showed distinct response which not only confirmed the detection of different types of damages i.e. compression or tensile but also, quantified the induced damage by the intensity of the signal. Besides all, the offset in the change in resistance of fiber sensors according to their position, demonstrated the detection of damage propagation in the composite plate in both in-plane and through-thickness for dynamic loading and this detection was in milliseconds. Therefore, the fiber sensor in each position presented the detection of damage initiation, damage evolution, type of damage, and specified whether it was localized or overall throughout the sample. This study confirmed the

ability of the Nylon/Ag fiber sensor as a flexible reinforcement in composite materials for *in-situ* monitoring because of its perfect correlation with the dynamic failure mechanism of the sample. This confirmed the durability and stability of this sensor and this study can be further continued with different types of composite specimens such as unidirectional (UD) composites or under other dynamic configurations.

## ORCID iDs

Y Qureshi  <https://orcid.org/0000-0002-5500-8654>

M Tarfaoui  <https://orcid.org/0000-0002-4932-3447>

## References

- [1] Pang J W C and Bond I P 2005 A hollow fibre reinforced polymer composite encompassing self-healing and enhanced damage visibility *Compos. Sci. Technol.* **65** 1791–9
- [2] Dry C 1996 Procedures developed for self-repair of polymer matrix composite materials *Compos. Struct.* **35** 263–9
- [3] Dry C and McMillan W 1997 A novel method to detect crack location and volume in opaque and semi-opaque brittle materials *Smart Mater. Struct.* **6** 35–39
- [4] Benyahia H, Tarfaoui M, El Moumen A, Ouinas D and Hassoon O H 2018 Mechanical properties of offshoring polymer composite pipes at various temperatures *Composites B* **152** 231–40
- [5] Sassi S, Tarfaoui M and Yahia H B 2018 Thermomechanical behavior of adhesively bonded joints under out-of-plane dynamic compression loading at high strain rate *J. Compos. Mater.* **52** 4171–84
- [6] El Moumen A, Tarfaoui M, Benyahia H and Lafdi K 2019 Mechanical behavior of carbon nanotubes-based polymer composites under impact tests *J. Compos. Mater.* **53** 925–40
- [7] Hassoon O H, Tarfaoui M and Alaoui A E M 2017 An experimental investigation on dynamic response of composite panels subjected to hydroelastic impact loading at constant velocities *Eng. Struct.* **153** 180–90
- [8] Ihn J-B and Chang F-K 2008 Pitch-catch active sensing methods in structural health monitoring for aircraft structures *Struct. Health Monit.* **7** 5–9
- [9] Cho H and Lissenden C J 2012 Structural health monitoring of fatigue crack growth in plate structures with ultrasonic guided waves *Struct. Health Monit.* **11** 393–404
- [10] Saeedifar M, Najafabadi M A, Yousefi J, Mohammadi R, Toudeshky H H and Minak G 2017 Delamination analysis in composite laminates by means of Acoustic Emission and bi-linear/tri-linear Cohesive Zone Modeling *Compos. Struct.* **161** 505–12
- [11] Crivelli D *et al* 2015 Localisation and identification of fatigue matrix cracking and delamination in a carbon fibre panel by acoustic emission *Composites B* **74** 1–12
- [12] Wang S, Chung D D L and Chung J H 2005 Impact damage of carbon fiber polymer–matrix composites, studied by electrical resistance measurement *Composites A* **36** 1707–15
- [13] Woo S-C and Kim T-W 2014 High-strain-rate impact in Kevlar-woven composites and fracture analysis using acoustic emission *Composites B* **60** 125–36
- [14] Vorathin E, Hafizi Z M, Ghani S A C and Lim K S 2016 Real-time monitoring system of composite aircraft wings utilizing Fibre Bragg Grating sensor
- [15] Liu H, Zhang Z, Jia H, Zhang D, Liu Y and Leng J 2019 Real-time monitoring system for multi-MW scale wind blades using FBG sensors *Health Monitoring of Structural and Biological Systems XIII*, vol. 10972 pp 353–60
- [16] Jang B-W and Kim C-G 2019 Impact localization of composite stiffened panel with triangulation method using normalized magnitudes of fiber optic sensor signals *Compos. Struct.* **211** 522–9
- [17] Farrar C R and Worden K 2007 An introduction to structural health monitoring *Philos. Trans. R. Soc. Ser. A* **365** 303–15
- [18] Wang X and Chung D D L 1997 Real-time monitoring of fatigue damage and dynamic strain in carbon fiber polymer-matrix composite by electrical resistance measurement
- [19] Hoheneder J, Flores-Vivian I, Lin Z, Zilberman P and Sobolev K 2015 The performance of stress-sensing smart fiber reinforced composites in moist and sodium chloride environments *Composites B* **73** 89–95
- [20] Todoroki A, Yamada K, Mizutani Y, Suzuki Y and Matsuzaki R 2015 Impact damage detection of a carbon-fibre-reinforced-polymer plate employing self-sensing time-domain reflectometry *Compos. Struct.* **130** 174–9
- [21] Park J-M, Lee S-I and DeVries K L 2006 Nondestructive sensing evaluation of surface modified single-carbon fiber reinforced epoxy composites by electrical resistivity measurement *Composites B* **37** 612–26
- [22] Park J-M, Kwon D-J, Wang Z-J, Kim -J-J, Jang K-W and Devries K L 2014 New method for interfacial evaluation of carbon fiber/thermosetting composites by wetting and electrical resistance measurements *J. Adhes. Sci. Technol.* **28** 1677–86
- [23] Wang Z-J *et al* 2013 Mechanical and interfacial evaluation of CNT/polypropylene composites and monitoring of damage using electrical resistance measurements *Compos. Sci. Technol.* **81** 69–75
- [24] Seo D-C and Lee -J-J 1999 Damage detection of CFRP laminates using electrical resistance measurement and neural network *Compos. Struct.* **47** 525–30
- [25] Abry J C, Bocharard S, Chateauminois A, Salvia M and Giraud G 1999 In situ detection of damage in CFRP laminates by electrical resistance measurements *Compos. Sci. Technol.* **59** 925–35
- [26] Swait T J, Jones F R and Hayes S A 2012 A practical structural health monitoring system for carbon fibre reinforced composite based on electrical resistance *Compos. Sci. Technol.* **72** 1515–23
- [27] Wen J, Xia Z and Choy F 2011 Damage detection of carbon fiber reinforced polymer composites via electrical resistance measurement *Composites B* **42** 77–86
- [28] Grammatikos S A and Paipetis A S 2012 On the electrical properties of multi scale reinforced composites for damage accumulation monitoring *Composites B* **43** 2687–96
- [29] Cagán J, Pelant J, Kyncl M, Kadlec M and Michalcová L 2019 Damage detection in carbon fiber–reinforced polymer composite via electrical resistance tomography with Gaussian anisotropic regularization *Struct. Health Monit.* **0** 1475921718820013
- [30] Johnson T M, Fullwood D T and Hansen G 2012 Strain monitoring of carbon fiber composite via embedded nickel nano-particles *Composites B* **43** 1155–63
- [31] Al-Dahawi A, Öztürk O, Emami F, Yıldırım G and Şahmaran M 2016 Effect of mixing methods on the electrical properties of cementitious composites incorporating different carbon-based materials *Constr. Build. Mater.* **104** 160–8
- [32] Eswaraiyah V, Balasubramaniam K and Ramaprabhu S 2011 Functionalized graphene reinforced thermoplastic nanocomposites as strain sensors in structural health monitoring *J. Mater. Chem.* **21** 12626–8

- [33] Grunlan J C, Gerberich W W and Francis L F 2001 Electrical and mechanical behavior of carbon black-filled poly (vinyl acetate) latex-based composites *Polym. Eng. Sci.* **41** 1947–62
- [34] Knite M, Teteris V, Kiploka A and Kaupuzs J 2004 Polyisoprene-carbon black nanocomposites as tensile strain and pressure sensor materials *Sensors Actuators A* **110** 142–9
- [35] Sandler J K W, Kirk J E, Kinloch I A, Shaffer M S P and Windle A H 2003 Ultra-low electrical percolation threshold in carbon-nanotube-epoxy composites *Polymer* **44** 5893–9
- [36] Bauhofer W and Kovacs J Z 2009 A review and analysis of electrical percolation in carbon nanotube polymer composites *Compos. Sci. Technol.* **69** 1486–98
- [37] Heeder N, Shukla A K, Chalivendra V, Yang S C and Park K 2012 Electrical response of carbon nanotube reinforced nanocomposites under static and dynamic loading *Exp. Mech.* **52** 315–22
- [38] Isaac-Medina B K S, Alonzo-García A and Avilés F 2019 Electrical self-sensing of impact damage in multiscale hierarchical composites with tailored location of carbon nanotube networks *Struct. Health Monit.* **18** 806–18
- [39] Rocker S N, Shirodkar N, McCoy T A and Seidel G D 2019 Electro-mechanical response of polymer bonded surrogate energetic materials with carbon nanotube sensing networks for structural health monitoring applications *Mechanics of Composite, Hybrid and Multifunctional Materials* (New York, USA: Springer International Publishing) **5** 185–93
- [40] Proper A, Zhang W, Bartolucci S F, Oberai A A and Koratkar N A 2009 In-situ detection of impact damage in composites using carbon nanotube sensor networks
- [41] Viets C, Kaysser S and Schulte K 2014 Damage mapping of GFRP via electrical resistance measurements using nanocomposite epoxy matrix systems *Composites B* **65** 80–88
- [42] Naghashpour A and Van Hoa S 2015 A technique for real-time detecting, locating, and quantifying damage in large polymer composite structures made of carbon fibers and carbon nanotube networks *Struct. Health Monit.* **14** 35–45
- [43] Gao L, Chou T-W, Thostenson E T, Zhang Z and Coulaud M 2011 In situ sensing of impact damage in epoxy/glass fiber composites using percolating carbon nanotube networks *Carbon* **49** 3382–5
- [44] Lim M-J, Lee H K, Nam I-W and Kim H-K 2017 Carbon nanotube/cement composites for crack monitoring of concrete structures *Compos. Struct.* **180** 741–50
- [45] Christian B 2000 Next generation structural health monitoring and its integration into aircraft design. *Int. J. Syst. Sci.* **31** 1333–49
- [46] Garcia C and Trendafilova I 2019 Triboelectric sensor as a dual system for impact monitoring and prediction of the damage in composite structures *Nano Energy* **60** 527–35
- [47] Martins A T, Aboura Z, Harizi W, Laksimi A and Hamdi K 2019 Structural health monitoring by the piezoresistive response of tufted reinforcements in sandwich composite panels *Compos. Struct.* **210** 109–17
- [48] Seyedin S, Razal J M, Innis P C, Jeiranikhameneh A, Beirne S and Wallace G G 2015 Knitted strain sensor textiles of highly conductive all-polymeric fibers *ACS Appl. Mater. Interfaces* **7** 21150–8
- [49] Trifigny N, Kelly F M, Cochrane C, Boussu F, Koncar V and Soulat D 2013 PEDOT: PSS-based piezo-resistive sensors applied to reinforcement glass fibres for in situ measurement during the composite material weaving process. *Sensors* **13** 10749–64
- [50] Jerkovic I, Koncar V and Grancaric A 2017 New textile sensors for in situ structural health monitoring of textile reinforced thermoplastic composites based on the conductive poly(3,4-ethylenedioxythiophene)-poly(styrenesulfonate) polymer complex *Sensors* **17** 2297
- [51] Cheng H, Dong Z, Hu C, Zhao Y, Hu Y, Qu L, Chen N and Dai L 2013 Textile electrodes woven by carbon nanotube-graphene hybrid fibers for flexible electrochemical capacitors *Nanoscale* **5** 3428
- [52] Nauman S, Cristian I, Boussu F and Koncar V 2013 *Smart Sensors for Industrial Applications. Part V Piezoresistive, Wireless, and Electrical Sensors* (USA: K. Iniewski)
- [53] Wang S, Xuan S, Liu M, Bai L, Zhang S, Sang M, Jiang W and Gong X 2017 Smart wearable kevlar-based safeguarding electronic textile with excellent sensing performance. *Soft Matter*. **13** 2483–91
- [54] Nag-Chowdhury S, Bellégou H, Pillin I, Castro M, Longrais P and Feller J F 2018 Coussou investigation of damage in composites with embedded quantum resistive strain sensors (sQRS), acoustic emission (AE) and digital image correlation (DIC) *Compos. Sci. Technol.* **160** 79–85
- [55] Cai G, Yang M, Xu Z, Liu J, Tang B and Wang. X 2017 Flexible and wearable strain sensing fabrics *Chem. Eng. J.* **325** 396–403
- [56] Yang H *et al* 2018 Highly sensitive and stretchable graphene-silicone rubber composites for strain sensing *Compos. Sci. Technol.* **167** 371–8
- [57] Hu N, Karube Y, Arai M, Watanabe T, Yan C and Li. Y 2010 Investigation on sensitivity of polymer/carbon nanotube composite strain sensor. *Carbon* **48** 680–7
- [58] Hu N, Fukunaga H, Atobe S, Liu Y and Li. J 2011 Piezoresistive strain sensors made from carbon nanotubes based polymer nanocomposites *Sensors* **11** 10691–723
- [59] Theodosiou T C and Saravanos D A 2010 Numerical investigation of mechanisms affecting the piezoresistive properties of CNT-doped polymers using multi-scale models *Compos. Sci. Technol.* **70** 1312–20
- [60] Wang G, Wang Y, Zhang P, Zhai Y, Luo Y, Li L and Luo S 2018 Structure dependent properties of carbon nanomaterials enabled fiber sensors for in situ monitoring of composites. *Compos. Struct.* **195** 36–44
- [61] Murray A R, Kisin E, Leonard S S, Young S H, Kommineni C, Kagan V E, Castranova V and Shvedova A A 2009 Oxidative stress and inflammatory response in dermal toxicity of single-walled carbon nanotubes. *Toxicology*. **257** 161–71
- [62] Kinkeldei T, Denier C, Zysset C, Muenzenrieder N and Troester. G 2013 2D thin film temperature sensors fabricated onto 3D nylon yarn surface for smart textile applications *Res. J. Text. Apparel* **17** 16–20
- [63] Xie J, Long H and Miao M 2016 High sensitivity knitted fabric strain sensors *Smart Mater. Struct.* **25** 105008
- [64] Ryu D, Loh K J, Ireland R, Karimzada M, Yaghmaie F and Gusman A M 2011 In situ reduction of gold nanoparticles in PDMS matrices and applications for large strain sensing *Smart Struct. Syst.* **8** 471–86
- [65] Wang R X, Tao X M, Wang Y, Wang G F and Shang. S M 2010 Microstructures and electrical conductance of silver nanocrystalline thin films on flexible polymer substrates. *Surf. Coat. Technol.* **204** 1206–10
- [66] Kim K-S *et al* 2018 Revisiting the thickness reduction approach for near-foldable capacitive touch sensors based on a single layer of Ag nanowire-polymer composite structure *Compos. Sci. Technol.* **165** 58–65
- [67] Atalay O, Tuncay A, Husain M D and Kennon W R 2016 Comparative study of the weft-knitted strain sensors *J. Ind. Text.* **46** 1212–40
- [68] Atwa Y, Maheshwari N and Goldthorpe. I A 2015 Silver nanowire coated threads for electrically conductive textiles. *J. Mater. Chem. C* **3** 3908–12
- [69] Qureshi Y, Tarfaoui M, Lafdi K K and Lafdi K 2019 Nanotechnology and development of strain sensor for

damage detection *Advances in Structural Health Monitoring* (London, UK: InTech Open)

- [70] Qureshi Y, Tarfaoui M, Lafdi K K and Lafdi K 2019 Real-time strain monitoring performance of flexible Nylon/Ag conductive fiber *Sensors Actuators A* **295** 612–22
- [71] Qureshi Y, Tarfaoui M, Lafdi K K and Lafdi K 2020 Real-time strain monitoring and damage detection of composites in different directions of the applied load using a microscale flexible Nylon/Ag strain sensor *Struct. Health Monit.* **19** 885–901
- [72] Qureshi Y, Tarfaoui M, Lafdi K K and Lafdi K 2019 Development of microscale flexible nylon/Ag strain sensor wire for real-time monitoring and damage detection in composite structures subjected to three-point bend test *Compos. Sci. Technol.* **181** 107693
- [73] Qureshi Y, Tarfaoui M, Lafdi K K and Lafdi K 2020 In-situ monitoring, identification and quantification of strain deformation in composites under cyclic flexural loading using Nylon/Ag fiber sensor *IEEE Sens. J.* **20** 1